

Supplement of

Formation and Loss of Light Absorbance by Phenolic Aqueous SOA by OH and an Organic Triplet Excited State

Stephanie Arciva¹, Lan Ma^{1a}, Camille Mavis^{1b}, Chrystal Guzman^{1c}, and Cort Anastasio¹

¹Department of Land, Air and Water Resources, University of California, Davis, One Shields Avenue, Davis, CA 95616-8627, USA

^aNow at: SGS-CSTC Standards Technical Services Co. Ltd., Hangzhou, Zhejiang Province, 310052, China

^bNow at: Department of Atmospheric Science, Colorado State University, Fort Collins, CO, 80521, USA

^cNow at: Department of Pharmacology, University of Washington, Seattle, WA, 98195, USA

Submitted to Atmospheric Chemistry and Physics on 15 November 2023

Correspondence to: Cort Anastasio (canastasio@ucdavis.edu)

Table of Contents

Table S1. Sampling time for ArOH oxidation reactions.....	3
Table S2. Molar absorptivities for six highly substituted ArOH.....	4
Table S3. ArOH decay kinetics by •OH and direct photodegradation.....	11
Table S4. ArOH decay kinetics by ³ C* and direct photodegradation.....	12
Table S5. aqSOA Mass Yields for highly substituted ArOH.....	13
Table S6. MAC _{ArOH} and MAC _{aqSOA,t1} for ArOH with •OH and ³ C*.....	14
Table S7. Fraction of rate of sunlight absorption (<i>R</i> _{abs}), AAE _{300-400nm} and log ₁₀ (MAC ₄₀₅) for ArOH with •OH and ³ C*.....	15
Table S8. Experimental and normalized <i>k'</i> _{Rabs}	17
Table S9. •OH concentrations in experimental solutions and ambient conditions.....	18
Table S10. ³ C* concentrations in experimental solutions and ambient conditions.....	19
Figure S1. Experimental and simulated actinic flux.....	20
Figure S2. ArOH oxidation kinetics with •OH and ³ C*.....	21
Figure S3. Molar absorptivities for six highly substituted ArOH.....	22
Figure S4. Absorbance measurements for mixtures during •OH reactions.....	23
Figure S5. Absorbance measurements for mixtures during ³ C* reactions.....	24
Figure S6. MAC for VAL, FA, and SyrAcid.....	25
Figure S7. Rates of sunlight absorption for VAL, FA, and SyrAcid.....	26
Figure S8. aqSOA light absorption decay kinetics for TYR, GA, and SA.....	27
Figure S9. aqSOA light absorption decay kinetics for VAL, FA, and SyrAcid.....	28
Figure S10. Lifetime of phenolic BrC for •OH and ³ C* reactions in clouds/drops and ALW.....	29
Section S1. Absorbance correction and MAC _{ArOH} determination.....	30

Table S1. Sampling time for ArOH oxidation reactions. Reaction times indicate approximately one, two, and three half-lives (i.e., $t_{1/2}$, $2t_{1/2}$, and $3t_{1/2}$) unless noted otherwise. ArOH concentrations were 100 μM except as marked. For $\bullet\text{OH}$ reactions, the H_2O_2 concentration was 5 mM, except for FA, SyrAcid and SA, which had 10 mM H_2O_2 . For $^3\text{C}^*$ reactions, solutions contained 10 μM DMB, except for tyrosol, which had 5 μM DMB.

Reaction Condition	$\bullet\text{OH}$ Reaction (min)	$^3\text{C}^*$ Reaction (min)
Tyrosol (TYR)	110	150
$t_{1/2}$	155	300
	235	450
$2 t_{1/2}$	295	600 ($0.85t_{1/2}$)
	365	750
$3 t_{1/2}$	415	1424 ($2t_{1/2}$)
Guaiacylacetone (GA)	70	90
$t_{1/2}$	140	200
	215	300
$2 t_{1/2}$	285	400
	330	520
$3 t_{1/2}$	385	640
Vanillyl alcohol (VAL)	60	90
$t_{1/2}$	143	130
	193	250
$2 t_{1/2}$	258	432
	323	610
$3 t_{1/2}$	378	1184 ($3.4t_{1/2}$)
Ferulic acid (FA) (50 μM)	60	120
$t_{1/2}$	140	240 ($0.43t_{1/2}$)
	210	440
$2 t_{1/2}$	280	680 ($1.6t_{1/2}$)
	350	-
$3 t_{1/2}$	420	1170 ($3.8t_{1/2}$)
Syringic acid (SyrAcid) (50 μM)	20	24
$t_{1/2}$	45	48
	70	72
$2 t_{1/2}$	85	96
	100	119
$3 t_{1/2}$	120	131
Syringylacetone (SA) (50 μM)	20	27
$t_{1/2}$	40	54
	60	81
$2 t_{1/2}$	76	108 ($2.2t_{1/2}$)
	88	135
$3 t_{1/2}$	98	157 ($3.5t_{1/2}$)

Table S2. Molar absorptivities for highly substituted ArOH. Base-10 molar absorption coefficients (ϵ) for aqueous ArOH determined from five different solutions of ArOH (25 μ M, 100 μ M, 500 μ M, 1.0 mM, and 2.0 mM) in a 1 cm cell. Plots are shown in Figure S3.

Wave-length (nm)	TYR	GA	VAL	<i>trans</i> -FA ^a		<i>cis</i> -FA ^a		SyrAcid ^b		SA
				pH 5	pH 2	pH 5	pH 2	pH 5	pH 2	
200	12500	36200	43900	11500	8460	18400	15900	24000	15500	44200
201	9690	35400	43200	11600	8350	18300	15700	24300	15900	45200
202	7890	33400	40000	11700	8170	18300	15000	24900	16700	46600
203	7030	30700	37300	11800	7990	18400	14300	25500	17400	47300
204	6240	27700	33600	12000	7840	18500	13700	26300	18200	47500
205	5790	24200	29300	12200	7730	18800	13000	27000	19100	46700
206	5540	21100	24600	12500	7650	18900	12400	27700	19900	45100
207	5490	18400	20400	12800	7640	18900	11800	28200	20700	42700
208	5490	16000	16500	13200	7680	18900	11200	28700	21500	39800
209	5560	14100	13300	13600	7820	18900	10800	29100	22200	36500
210	5640	12600	10700	14100	8020	18900	10500	29300	22900	33300
211	5750	11300	8960	14500	8260	18800	10200	29400	23600	30300
212	5910	10400	7710	14900	8500	18600	10000	29500	24200	27500
213	6010	9630	6940	15200	8750	18500	9890	29600	24800	25100
214	6090	9050	6450	15500	9000	18300	9720	29400	25200	22900
215	6200	8580	6170	15700	9220	18000	9570	29200	25600	21000
216	6290	8180	6010	15900	9390	17600	9430	28700	25900	19400
217	6470	7860	5950	15900	9520	17200	9270	27900	26100	18000
218	6630	7590	5960	15800	9590	16700	9090	26900	26000	16900
219	6830	7350	6010	15700	9550	16200	8920	25600	25700	15900
220	6970	7160	6070	15300	9400	15600	8740	23500	25100	15000
221	7030	6970	6150	14900	9130	15000	8550	21800	24200	14300
222	7000	6800	6240	14500	8800	14400	8340	20100	23000	13600
223	6800	6640	6340	14100	8490	13800	8130	18000	21500	13000
224	6510	6480	6430	13800	8280	13200	7960	15600	19600	12500
225	6050	6330	6520	13700	8150	12600	7830	14100	17500	12100
226	5470	6180	6590	13600	8100	12100	7720	11800	15300	11700
227	4820	6030	6630	13600	8150	11600	7630	10200	13100	11300
228	4160	5880	6620	13600	8250	11100	7550	8150	11100	10900
229	3560	5710	6560	13500	8370	10700	7490	7080	9370	10600
230	2910	5520	6430	13500	8510	10300	7410	6180	7590	10200
231	2320	5290	6230	13400	8650	9910	7350	5450	6240	9870
232	1790	5040	5980	13200	8750	9520	7280	4880	5130	9530

Wave-length (nm)	TYR	GA	VAL	<i>trans</i> -FA		<i>cis</i> -FA		SyrAcid		SA
				pH 5	pH 2	pH 5	pH 2	pH 5	pH 2	
233	1390	4760	5670	13000	8830	9160	7190	4450	4230	9160
234	1070	4480	5300	12800	8860	8830	7090	4130	3460	8770
235	800	4170	4890	12600	8860	8510	6980	3900	2920	8350
236	605	3850	4450	12300	8830	8210	6860	3740	2510	7920
237	450	3520	3920	12000	8780	7920	6730	3650	2200	7480
238	344	3200	3450	11700	8710	7640	6590	3610	2000	7010
239	266	2890	3000	11400	8640	7410	6450	3630	1880	6520
240	208	2580	2550	11000	8550	7210	6300	3700	1820	6050
241	171	2300	2140	10600	8440	7050	6140	3820	1820	5590
242	146	2050	1750	10200	8300	6930	5980	3970	1870	5110
243	132	1810	1430	9730	8120	6830	5800	4170	1960	4650
244	125	1620	1140	9270	7900	6780	5630	4380	2080	4230
245	124	1450	925	8700	7640	6780	5440	4630	2240	3830
246	129	1310	752	8240	7360	6800	5240	4900	2410	3470
247	137	1190	619	7780	7040	6840	5060	5180	2610	3150
248	149	1090	517	7330	6690	6930	4870	5480	2840	2840
249	163	1010	445	6910	6320	7040	4700	5790	3080	2570
250	182	947	399	6510	5950	7160	4530	6090	3330	2350
251	203	895	372	6160	5560	7320	4350	6410	3610	2150
252	226	855	361	5860	5070	7490	4280	6710	3950	1980
253	258	827	363	5610	4690	7680	4100	7030	4270	1840
254	289	810	377	5410	4320	7890	3950	7330	4600	1720
255	327	804	402	5280	3990	8120	3840	7630	4950	1630
256	367	810	437	5210	3690	8370	3740	7900	5320	1550
257	416	827	480	5210	3460	8610	3670	8140	5700	1480
258	468	856	533	5270	3270	8860	3630	8370	6090	1440
259	524	897	596	5400	3130	9090	3610	8550	6480	1420
260	583	949	667	5590	3060	9290	3620	8710	6870	1410
261	645	1010	747	5820	3040	9480	3640	8830	7250	1410
262	711	1080	835	6100	3060	9650	3680	8900	7750	1430
263	785	1170	933	6440	3120	9810	3760	8920	8120	1450
264	862	1270	1040	6810	3230	9930	3850	8910	8480	1480
265	944	1370	1150	7210	3370	10000	3920	8850	8810	1520
266	1030	1480	1260	7630	3540	10100	4020	8760	9090	1560
267	1100	1590	1400	8060	3730	10200	4140	8630	9350	1610
268	1180	1710	1520	8490	3960	10200	4260	8470	9590	1640
269	1240	1830	1650	8850	4190	10100	4390	8280	9790	1680
270	1300	1950	1770	9270	4440	10100	4490	8080	9960	1710
271	1360	2080	1890	9720	4710	9940	4590	7860	10000	1740
272	1420	2200	2020	10200	4990	9790	4670	7620	10100	1770

Wave-length (nm)	TYR	GA	VAL	<i>trans</i> -FA		<i>cis</i> -FA		SyrAcid		SA
				pH 5	pH 2	pH 5	pH 2	pH 5	pH 2	
273	1480	2320	2140	10600	5420	9580	4770	7360	10200	1780
274	1530	2440	2260	11100	5730	9350	4890	7100	10200	1790
275	1570	2550	2370	11500	6050	9100	5020	6840	10200	1800
276	1570	2660	2460	11900	6380	8850	5140	6570	10200	1800
277	1540	2750	2520	12300	6730	8610	5240	6310	10100	1810
278	1480	2820	2570	12700	7080	8370	5310	6050	10000	1810
279	1420	2860	2590	13100	7430	8140	5380	5810	9960	1820
280	1360	2880	2570	13400	7780	7940	5450	5560	9800	1820
281	1330	2870	2520	13700	8110	7750	5550	5320	9620	1810
282	1290	2830	2440	14000	8430	7580	5660	5080	9430	1790
283	1210	2780	2360	14200	8740	7430	5780	4840	9220	1750
284	1080	2710	2290	14400	9030	7310	5870	4610	9010	1700
285	897	2640	2180	14600	9300	7210	5930	4370	8790	1630
286	708	2540	2000	14700	9550	7130	5970	4130	8560	1570
287	526	2410	1750	14800	9780	7070	6020	3900	8340	1520
288	376	2240	1450	14900	9990	7020	6090	3670	8110	1480
289	255	2030	1100	14900	10200	7000	6170	3400	7870	1460
290	170	1800	836	14900	10500	6990	6260	3180	7550	1440
291	112	1580	607	14900	10700	6990	6300	2960	7300	1430
292	71	1370	424	14800	10800	7000	6330	2740	7040	1420
293	45.3	1200	289	14700	11000	7020	6380	2520	6770	1420
294	28	1050	192	14700	11100	7040	6440	2310	6490	1410
295	17.7	924	125	14600	11200	7040	6490	2100	6190	1400
296	11	828	81.5	14500	11200	7050	6540	1900	5890	1400
297	6.7	748	52.5	14500	11300	7040	6570	1700	5570	1400
298	4.0	682	34.1	14500	11300	7020	6640	1500	5230	1400
299	2.5	628	22.1	14500	11400	6980	6690	1320	4900	1390
300	1.5	582	14.4	14600	11400	6920	6730	1210	4560	1380
301	0.93	542	9.3	14700	11500	6840	6770	1050	4200	1370
302	0.56	508	6.1	14800	11500	6750	6810	909	3800	1360
303	0.35	478	3.9	14900	11600	6650	6860	787	3450	1350
304	0.23	452	2.6	15000	11700	6530	6880	677	3120	1330
305	0.14	428	1.7	15100	11800	6370	6900	581	2800	1320
306	0	407	1.3	15200	11900	6210	6910	498	2480	1310
307		387	0.98	15400	12100	6030	6920	426	2180	1300
308		369	0.75	15500	12200	5850	6940	364	1910	1280
309		353	0.57	15600	12300	5670	6960	311	1660	1260
310		338	0.43	15700	12500	5470	6980	264	1430	1240
311		323	0.33	15800	12700	5260	6990	222	1220	1220
312		310	0.25	15800	12900	5040	6970	189	1030	1200

wave length (nm)	TYR	GA	VAL	<i>trans</i> -FA		<i>cis</i> -FA		SyrAcid		SA
				pH 5	pH 2	pH 5	pH 2	pH 5	pH 2	
313		297	0.19	15800	13100	4800	6920	156	889	1170
314		284	0.15	15800	13300	4550	6880	127	739	1140
315		273	0.11	15700	13500	4310	6840	104	610	1110
316		263	0	15700	13600	4080	6790	81.8	496	1080
317		252		15500	13800	3850	6760	66.1	401	1060
318		242		15400	13900	3620	6700	52.8	323	1020
319		232		15100	14000	3440	6610	41.7	257	994
320		222		14900	14100	3270	6530	33.3	204	962
321		213		14600	14200	3110	6480	26.6	161	928
322		204		14300	14200	2970	6410	21.2	126	892
323		195		13800	14200	2850	6300	16.8	97.9	856
324		186		13400	14100	2740	6180	14.1	76.5	824
325		178		13000	14100	2640	6080	11.7	60.0	792
326		169		12500	13900	2570	5970	9.8	46.5	756
327		161		12000	13800	2500	5830	8.2	35.9	710
328		152		11500	13600	2430	5720	6.8	27.5	674
329		144		10900	13400	2370	5570	5.7	21.2	642
330		136		10400	13200	2290	5400	4.6	16.5	598
331		127		9770	12900	2220	5240	3.8	12.6	558
332		119		9180	12500	2150	5070	3.0	9.7	524
333		111		8610	12200	2100	4920	2.6	7.5	494
334		103		8050	11800	2070	4740	2.4	5.8	458
335		96		7500	11400	2030	4570	1.9	4.4	422
336		89.3		6950	11000	2000	4370	1.7	3.6	390
337		82.8		6410	10500	1940	4150	1.4	3.1	362
338		76.7		5910	9940	1890	3920	0.99	2.6	336
339		70.9		5440	9460	1810	3730	0.81	2.0	306
340		65.5		5000	8970	1730	3470	0.68	1.7	284
341		60.8		4610	8490	1640	3320	0.64	1.6	260
342		56.6		4240	8010	1570	3160	0.62	1.4	240
343		53.1		3890	7560	1490	3000	0.75	1.3	218
344		49.5		3560	7120	1420	2830	0.61	0	204
345		46.4		3270	6680	1340	2670	0.29		188
346		43.5		3000	6260	1260	2520	0.27		168
347		40.8		2740	5830	1190	2390	0.17		158
348		38.5		2510	5420	1150	2260	0		152
349		36.4		2290	4920	1100	2120			148
350		34.5		2090	4550	1050	1990			144
351		32.6		1890	4180	974	1860			138
352		30.8		1710	3810	898	1720			126
353		29.3		1530	3480	828	1590			118

wave length (nm)	TYR	GA	VAL	<i>trans</i> -FA		<i>cis</i> -FA		SyrAcid		SA
				pH 5	pH 2	pH 5	pH 2	pH 5	pH 2	
354		28.0		1380	3150	760	1470			122
355		26.5		1230	2850	692	1360			116
356		24.9		1100	2570	627	1250			108
357		23.6		977	2300	568	1150			106
358		22.4		870	2060	515	1050			96
359		21.4		771	1830	467	960			86
360		20.2		682	1630	424	873			88
361		19.2		602	1450	381	789			84
362		18.8		533	1290	342	719			72
363		18.1		471	1150	306	657			68
364		17.1		417	1010	275	601			74
365		16.4		366	896	246	545			70
366		15.8		322	788	221	489			68
367		15.0		281	690	196	437			72
368		14.2		244	601	173	388			72
369		13.4		212	523	153	350			70
370		12.7		184	454	135	316			66
371		12.4		159	393	118	281			62
372		11.9		137	337	103	248			60
373		11.3		118	290	90.7	218			60
374		10.6		101	250	79.6	193			56
375		10.1		86.6	213	69.2	171			52
376		9.6		73.8	181	60.3	153			54
377		9.1		63.1	154	52.3	135			54
378		8.7		54.2	131	45.3	119			44
379		8.5		46.8	113	39.7	105			44
380		8.2		40.3	97	34.7	92			46
381		7.7		34.4	83	30.1	80			46
382		7.3		29.5	71	26.3	69			38
383		7.0		25.6	60	22.5	62			34
384		6.7		22	51	19.1	55			40
385		6.5		19	43	16.7	51			40
386		6.3		16.2	37	14.8	44			38
387		5.9		13.4	31	12.3	37			34
388		5.7		11	26	10.6	33			26
389		5.4		9.3	22	8.4	28			30
390		5.1		8.0	18	6.7	22			28
391		5.0		0	0	0	0			22
392		4.9								20
393		4.6								18
394		4.2								20

wave length (nm)	TYR	GA	VAL	<i>trans</i> -FA		<i>cis</i> -FA		SyrAcid		SA
				pH 5	pH 2	pH 5	pH 2	pH 5	pH 2	
395		3.9								18
396		3.9								16
397		3.8								12
398		3.6								12
399		3.3								14
400		3.1								12
401		3.1								0
402		3.0								
403		2.9								
404		2.8								
405		2.7								
406		2.6								
407		2.5								
408		2.4								
409		2.2								
410		2.0								
411		2.0								
412		2.0								
413		1.8								
414		1.7								
415		1.7								
416		1.7								
417		1.7								
418		1.6								
419		1.5								
420		1.5								
421		1.5								
422		1.4								
423		1.2								
424		1.2								
425		1.2								
426		1.2								
427		1.1								
428		1.1								
429		1.0								
430		1.0								
431		0.96								
432		0.80								
433		0.69								
434		0.67								
435		0.70								
436		0.69								

Wave-length (nm)	TYR	GA	VAL	<i>trans</i> -FA		<i>cis</i> -FA		SyrAcid		SA
				pH 5	pH 2	pH 5	pH 2	pH 5	pH 2	
437		0.61								
438		0.60								
439		0.70								
440		0.75								
441		0.70								
442		0.52								
443		0.49								
444		0.53								
445		0.44								
446		0.37								
447		0.41								
448		0.36								
449		0.32								
450		0.26								
451		0.26								
452		0.28								
453		0.26								
454		0.26								
455		0.20								
456		0.06								
457		0.04								
458		0.10								
459		0.11								
460		0.08								
461		0.04								
462		0								

^a Ferulic acid has a carboxylic acid group with a pK_a of 4.6 (Erdemgil et al. 2007). Molar absorption coefficients of *trans*- and *cis*-ferulic acid were determined by first measuring the *trans* isomer. As noted above, we prepared five different solutions of *trans*-ferulic acid, which is the isomer received from the vendor. We measured the absorbance of these initial solutions and determined the molar absorptivity directly for *trans*-FA. Next, we illuminated each of the five solutions individually for 20 mins to equilibrate the photoisomerization of FA. We quantified the fraction of each isomer using HPLC and measured the absorbance of the solution after illumination. Then, we determined the molar absorption coefficients of *cis*-FA by $\epsilon_{cis-FA} = \frac{Abs_{corrected}}{l \times [cis-FA]}$, where $Abs_{corrected}$ is the absorbance of the solution corrected to remove the absorbance contribution from *trans*-FA, l is the cell path length (1 cm), and $[cis-FA]$ is the concentration of the *cis*-isomer in M, as determined by HPLC.

^b Syringic acid has a carboxylic group with a pK_a of 4.2 (Erdemgil et al. 2007).

Table S3. ArOH Decay Kinetics by $\bullet\text{OH}^{\text{a}}$

Phenol	$k'_{\text{light}}^{\text{b}}$ (10^{-4} s^{-1})	$j_{\text{ArOH}}^{\text{c}}$ (10^{-4} s^{-1})	$k'_{\text{ArOH}}^{\text{d}}$ (10^{-4} s^{-1})	$[\bullet\text{OH}]_{\text{exp}}^{\text{e}}$ (10^{-15} M)
TYR	0.89	≈ 0	1.3	8.9
GA	0.88	≈ 0	1.2	8.2
VAL	0.96	≈ 0	1.3	8.4
FA ^f	0.91	0.041	1.2	6.5
SyrAcid	2.9	0.45	3.6	18
SA	3.4	0.65	4.1	17

^a Concentrations of reactants are in Table S1. The photolysis rate constant for 2-nitrobenzaldehyde, our chemical actinometer, was measured once during our $\bullet\text{OH}$ experiments, with a value of $5.0 \times 10^3 \text{ s}^{-1}$.

^b Experimentally determined pseudo-first-order rate constant for the decay of ArOH by $\bullet\text{OH}$, determined as the negative of the slope of $\ln([\text{ArOH}]/[\text{ArOH}]_0)$ versus reaction time (Figure S2).

^c Previously measured photolysis rate constants under midday, Davis winter-solstice sunlight for ArOH in simulated sunlight from Arciva et al. (2022).

^d Corrected pseudo-first-order decay constant for ArOH loss by $\bullet\text{OH}$, determined by $k'_{\text{ArOH}} = \left[\left(\frac{k'_{\text{light}}}{j_{2\text{NB},\text{win}}} \right) \times j_{2\text{NB},\text{win}} \right] - j_{\text{ArOH}}$. We normalized values to sunlight conditions at midday on the winter solstice at Davis ($j_{2\text{NB},\text{win}} = 0.0070 \text{ s}^{-1}$) (Anastasio and McGregor 2001).

^e Steady-state concentrations of $\bullet\text{OH}$ in experimental solutions (normalized to winter-solstice sunlight) estimated by $[\bullet\text{OH}] = \frac{k'_{\text{ArOH}}}{k_{\text{ArOH}+\text{OH}}}$, where $k_{\text{ArOH}+\text{OH}}$ ($\text{M}^{-1} \text{ s}^{-1}$) is the second-order rate constant of ArOH with $\bullet\text{OH}$ (Arciva et al., 2022).

^f Values for FA represent a weighted average between the *cis* and *trans* isomers.

Table S4. ArOH Decay Kinetics by $^3\text{C}^*$

Phenol	$j_{2\text{NB}}^{\text{a}}$ (10^{-4} s^{-1})	$k'_{\text{light}}^{\text{b}}$ (10^{-4} s^{-1})	$k'_{\text{ArOH}}^{\text{c}}$ (10^{-4} s^{-1})	$[^3\text{C}^*]_{\text{exp}}^{\text{d}}$ (10^{-14} M)
TYR	59	0.16	0.19	4.0
GA	65	0.50	0.54	2.9
VAL	100	0.31	0.21	1.2
FA ^e	61	0.37	0.38	4.6
SyrAcid	61	2.4	2.4	11
SA	61	2.6	2.4	8.7

^a Photolysis rate constant for 2-nitrobenzaldehyde, a chemical actinometer, on the day of an aqSOA experiment.

^b Pseudo-first-order rate constant for the decay of ArOH by oxidizing triplets, determined from the slope of the plot $\ln([\text{ArOH}]/[\text{ArOH}]_0)$ versus reaction time (Figure S2).

^c Corrected pseudo-first-order decay of ArOH by $^3\text{C}^*$, determined by $k'_{\text{ArOH}} = \left[\left(\frac{k'_{\text{light}}}{j_{2\text{NB}}} \right) \times j_{2\text{NB},\text{win}} \right] - j_{\text{ArOH}}$. Values of j_{ArOH} , the direct photodegradation rate constant for each phenol normalized to Davis winter-solstice sunlight, are in Table S2. k'_{ArOH} values are normalized to sunlight conditions at midday on the winter solstice at Davis ($j_{2\text{NB},\text{win}} = 0.0070 \text{ s}^{-1}$) (Anastasio and McGregor 2001).

^d Steady-state concentration of $^3\text{C}^*$ in experimental solutions (normalized to winter-solstice sunlight) estimated by $[^3\text{C}^*] = \frac{k'_{\text{ArOH}}}{k_{\text{ArOH}+^3\text{C}^*}}$, where $k_{\text{ArOH}+^3\text{C}^*}$ ($\text{M}^{-1} \text{ s}^{-1}$) as the second-order rate constant of ArOH with $^3\text{C}^*$ (Ma et al., 2021).

^e Values for FA represent a weighted average between the *cis* and *trans* isomers.

Table S5. aqSOA Mass Yields for highly substituted ArOH

Compound	\bullet OH Reaction aqSOA Mass Yield ($\pm 1\sigma$) ^a	³ C* Reaction aqSOA Mass Yield ($\pm 1\sigma$) ^b
TYR	94.3 (± 3.6)	85.9 (± 3.9)
GA	65.5 (± 7.8)	84.5 (± 3.8)
VAL	73.7 (± 3.1)	59.0 (± 2.0)
FA	83.1 (± 6.1)	90.6 (± 13.8)
SyrAcid	63.8 (± 2.7)	78.5 (± 8.6)
SA	81.4 (± 4.9)	99.1 (± 7.9)
Avg ($\pm 1\sigma$)	82 (± 12)	83 (± 14)

^a AqSOA mass yields are an average of measurements of samples at one, two, and three half-lives (i.e., $t_{1/2}$, $2t_{1/2}$, $3t_{1/2}$) (Arciva et al., 2022).

^b AqSOA mass yields are an average of measurements of samples at one, two, and three half-lives (i.e., $t_{1/2}$, $2t_{1/2}$, $3t_{1/2}$) (Ma et al., 2021).

Table S6. MAC_{ArOH} and $MAC_{aqSOA,t1}$ for ArOH reacting with $\bullet OH$ or $^3C^*$. MAC values (in units of $m^2 g^{-1}$) at 300 nm for the parent ArOH (MAC_{ArOH}) and for the aqSOA at the first sampled time point ($MAC_{aqSOA,t1}$) with reaction time as marked. For aqSOA values, we subtracted the absorbance contribution from the reactants (i.e., unreacted ArOH and oxidant precursor).

		$\bullet OH$ Reaction	$^3C^*$ Reaction
Phenol	MAC_{ArOH}	$MAC_{aqSOA,t1}$	$MAC_{aqSOA,t1}$
TYR	0.00	0.63 (110 min)	1.7 (150 min)
GA	0.88	3.0 (70 min)	3.3 (90 min)
VAL	0.02	3.4 (60 min)	3.2 (90 min)
FA	9.0	4.4 (60 min)	5.5 (120 min)
SyrAcid	1.5	6.1 (20 min)	9.0 (24 min)
SA	1.7	5.1 (20 min)	6.0 (27 min)

Table S7. Light absorption characteristics of the aqSOA: Fraction of light absorption (R_{abs}) due to short wavelengths, $\text{AAE}_{300-400\text{nm}}$, and $\log_{10}(\text{MAC}_{405})$. Values are listed as a time series from top to bottom (with times shown in Table S1). R_{abs} data are shown in Figures 4 and S7.

Phenol	•OH Reactions			³ C* Reactions		
	Fraction of $R_{\text{abs,t1}}$ from wavelengths < 400 nm ^a	$\text{AAE}_{300-400\text{nm}}$ ^b	$\log_{10}(\text{MAC}_{405})$	Fraction of $R_{\text{abs,t1}}$ from wavelengths < 400 nm ^a	$\text{AAE}_{300-400\text{nm}}$ ^b	$\log_{10}(\text{MAC}_{405})$
TYR	0.23	8.8	-1.36	0.38	10.22	-1.05
	0.32	8.8	-1.25	0.37	8.43	-0.80
	0.40	8.7	-1.18	0.45	8.57	-0.83
	0.47	8.6	-1.17	0.39	7.53	-0.67
	0.48	8.6	-1.15	0.46	7.94	-0.76
	0.52	8.6	-1.16	0.53	7.63	-0.73
GA	0.48	9.1	-0.72	0.83	9.6	-0.77
	0.54	9.0	-0.79	0.78	8.7	-0.69
	0.54	8.9	-0.84	0.77	8.4	-0.69
	0.57	9.2	-0.93	0.76	8.3	-0.70
	0.59	9.3	-0.98	0.77	8.3	-0.72
	0.59	9.3	-1.04	0.77	8.3	-0.74
VAL	0.25	10.1	-0.76	0.16	7.5	-0.46
	0.37	9.5	-0.76	0.21	7.5	-0.46
	0.44	9.2	-0.78	0.31	7.2	-0.42
	0.49	9.1	-0.83	0.37	6.8	-0.36
	0.51	8.9	-0.89	0.41	6.8	-0.35
	0.54	8.9	-0.95	0.44	6.8	-0.36
FA	0.67	11	-0.75	0.74	12	-0.83
	0.68	11	-0.79	0.68	11	-0.72
	0.67	10	-0.80	0.71	11	-0.78
	0.68	10	-0.85	0.76	11	-0.84
	0.67	9.9	-0.90	0.71	10	-0.78
	0.68	9.6	-0.93			
SA	0.63	5.0	0.06	0.64	3.7	0.28
	0.67	5.2	-0.01	0.65	3.9	0.26
	0.67	5.3	-0.05	0.65	3.9	0.24
	0.66	5.3	-0.08	0.64	4.0	0.21
	0.67	5.6	-0.14	0.64	4.1	0.18
	0.67	5.7	-0.19	0.64	4.1	0.16
SyrAcid	0.70	15	-1.19	0.55	12	-0.54
	0.48	14	-1.02	0.53	11	-0.51
	0.45	14	-1.07	0.52	11	-0.54
	0.44	14	-1.10	0.49	11	-0.55
	0.41	13	-1.17	0.50	11	-0.58
	0.43	13	-1.31	0.50	11	-0.66

^a Fraction of the rate of sunlight absorption by aqSOA at the first illumination time point that is due to wavelengths below 400 nm.

^b Absorption Ångström exponent calculated using $AAE_{300-400nm} = -\frac{\ln \frac{MAC_{300}}{MAC_{400}}}{\ln \frac{300}{400}}$.

Table S8. Experimental and normalized k'_{Rabs} values.

Phenol	•OH Reactions		³ C* Reactions	
	$k'_{Rabs,exp}$ ^a (10 ⁻³ min ⁻¹)	k'_{Rabs} ^b (10 ⁻³ min ⁻¹)	$k'_{Rabs,exp}$ ^c (10 ⁻³ min ⁻¹)	k'_{Rabs} ^d (10 ⁻³ min ⁻¹)
TYR	0.74	1.0	0.080	0.095
GA	2.6	3.6	0.46	0.50
VAL	3.1	4.3	0.24	0.17
FA	1.7	2.4	0.0046	0.0053
SyrAcid	6.7	9.4	3.4	3.9
SA	4.9	6.9	2.4	2.8

^a Experimentally measured rate constant for loss of the rate of light absorption by •OH-derived aqSOA in the presence of •OH.

^b Corrected pseudo-first-order decay constant for the loss of light absorption by aqSOA in the presence of •OH determined by $k'_{Rabs} = \left[\left(\frac{k'_{Rabs,exp}}{j_{2NB}} \right) \times j_{2NB,win} \right]$. We normalized values to sunlight conditions at midday on the winter solstice at Davis ($j_{2NB,win} = 0.0070 \text{ s}^{-1}$) (Anastasio and McGregor 2001).

^c Experimentally measured rate constant for loss of the rate of light absorption by ³C*-derived aqSOA in the presence of ³C*.

^d Corrected pseudo-first-order decay constant for the loss of light absorption by aqSOA in the presence of ³C*, determined by $k'_{Rabs} = \left[\left(\frac{k'_{Rabs,exp}}{j_{2NB}} \right) \times j_{2NB,win} \right]$. We normalized values to sunlight conditions at midday on the winter solstice at Davis ($j_{2NB,win} = 0.0070 \text{ s}^{-1}$) (Anastasio and McGregor 2001).

Table S9. •OH concentrations and rate constants for loss of absorbance under experimental solutions and extrapolated to ambient conditions in aerosol liquid water (ALW) and cloud/fog drops (drop).

Phenol	[•OH] _{exp} ^a (10 ⁻¹⁵ M)	<i>k</i> ' _{Rabs} ^b (10 ⁻³ min ⁻¹)	[•OH] _{drop} / [•OH] _{exp} ^c (M / M)	<i>k</i> ' _{Rabs,drop} ^d (10 ⁻³ min ⁻¹)	[•OH] _{ALW} / [•OH] _{exp} ^e (M / M)	<i>k</i> ' _{Rabs,ALW} ^f (10 ⁻³ min ⁻¹)
TYR	8.9	1.0	1.2	0.88	0.61	0.46
GA	8.2	3.6	1.3	3.4	0.66	1.7
VAL	8.4	4.3	1.3	4.0	0.65	2.0
FA	6.5	2.4	1.6	2.8	0.84	1.4
SyrAcid	18	9.4	0.59	3.9	0.30	2.0
SA	17	6.9	0.65	3.2	0.33	1.6

^a •OH concentration calculated from the pseudo-first-order loss of ArOH for each experiment (Table S2). Values are normalized to Davis winter-solstice conditions and corrected for *j*_{ArOH}.

^b Experimentally determined rate constant for decay of the rate of light absorption by aqSOA determined by the plot of the natural log of the total rate of light absorption from 280 to 800 nm (Equation 2) versus reaction time.

^c Ratio of [•OH] estimated in fog drops to the •OH concentration in our experiment. Both conditions are normalized to midday winter-solstice sunlight in Davis. For fog drops we use the Ma et al. (2023) estimate of [•OH]_{drop} = 1.1 × 10⁻¹⁴ M for winter-spring PM extracts and a dilution condition typical of a clean fog (3 × 10⁻⁵ μg-PM / μg-water).

^d Estimated rate constant for loss of the rate of light absorption by aqSOA in a fog/cloud drop, determined as the measured (and sunlight-normalized) value of *k*'_{Rabs} multiplied by the ratio [•OH]_{drop} / [•OH]_{exp}.

^e Ratio of [•OH] estimated in aerosol liquid water to the •OH concentration in our experiment; both values are normalized to winter-solstice sunlight. We use an estimate of [•OH]_{ALW} = 5.5 × 10⁻¹⁵ M for 1 μg-PM / 1 μg-water for Davis winter-spring samples, which were significantly influenced by residential wood combustion, from Ma et al. (2023).

^f Estimated rate constant for loss of the rate of light absorption by aqSOA in ALW, determined as the measured (and sunlight-normalized) value of *k*'_{Rabs} multiplied by the ratio [•OH]_{ALW} / [•OH]_{exp}.

Table S10. $^3\text{C}^*$ concentrations and rate constants for loss of absorbance under experimental solutions and extrapolated to ambient conditions in aerosol liquid water (ALW) and cloud/fog drops (drop).

Phenol	$[\text{}^3\text{C}^*]_{\text{exp}}^{\text{a}}$ (10^{-14} M)	$k'_{\text{Rabs}}^{\text{b}}$ (10^{-3} min $^{-1}$)	$[\text{}^3\text{C}^*]_{\text{drop}} / [\text{}^3\text{C}^*]_{\text{exp}}^{\text{c}}$ (M / M)	$k'_{\text{Rabs,drop}}^{\text{d}}$ (10^{-3} min $^{-1}$)	$[\text{}^3\text{C}^*]_{\text{ALW}} / [\text{}^3\text{C}^*]_{\text{exp}}^{\text{e}}$ (M / M)	$k'_{\text{Rabs,ALW}}^{\text{f}}$ (10^{-3} min $^{-1}$)
TYR	4.0	0.095	0.92	0.074	20	1.6
GA	2.9	0.50	1.3	0.60	29	13
VAL	1.2	0.17	3.2	0.76	70	17
FA	4.6	0.0053	0.80	0.0036	18	0.082
SyrAcid	11	3.9	0.33	1.1	7.3	25
SA	8.7	2.8	0.42	1.0	9.4	23

^a $^3\text{C}^*$ concentration calculated from the pseudo-first-order loss of ArOH for each experiment (Table S2). Values are normalized to Davis winter-solstice conditions and corrected for j_{ArOH} .

^b Experimentally determined rate constant for decay of the rate of light absorption by aqSOA determined by the plot of the natural log of the total rate of light absorption from 280 to 800 nm (Equation 2) versus reaction time.

^c Ratio of $[\text{}^3\text{C}^*]$ estimated in fog drops to the $\bullet\text{OH}$ concentration in our experiments. Both values are normalized to winter-solstice sunlight. For fog drops we use the Ma et al. (2023) estimate of $[\text{}^3\text{C}^*]_{\text{drop}} = 3.7 \times 10^{-14}$ M for winter-spring PM extracts and a dilution condition typical of clean fog (3×10^{-5} $\mu\text{g-PM} / \mu\text{g-water}$).

^d Estimated rate constant for loss of the rate of light absorption by aqSOA in a fog/cloud drop, determined as the measured (and sunlight-normalized) value of k'_{Rabs} multiplied by the ratio $[\text{}^3\text{C}^*]_{\text{drop}} / [\text{}^3\text{C}^*]_{\text{exp}}$.

^e Ratio of $[\text{}^3\text{C}^*]$ estimated in aerosol liquid water to the $^3\text{C}^*$ concentration in our experiment; both values are normalized to winter-solstice sunlight. We use an estimate of $[\text{}^3\text{C}^*]_{\text{ALW}} = 8.2 \times 10^{-13}$ M for 1 $\mu\text{g-PM} / 1 \mu\text{g-water}$ for Davis winter-spring samples, which were significantly influenced by residential wood combustion, from Ma et al. (2023).

^f Estimated rate constant for loss of the rate of light absorption by aqSOA in ALW, determined as the measured (and sunlight-normalized) value of k'_{Rabs} multiplied by the ratio $[\text{}^3\text{C}^*]_{\text{ALW}} / [\text{}^3\text{C}^*]_{\text{exp}}$.

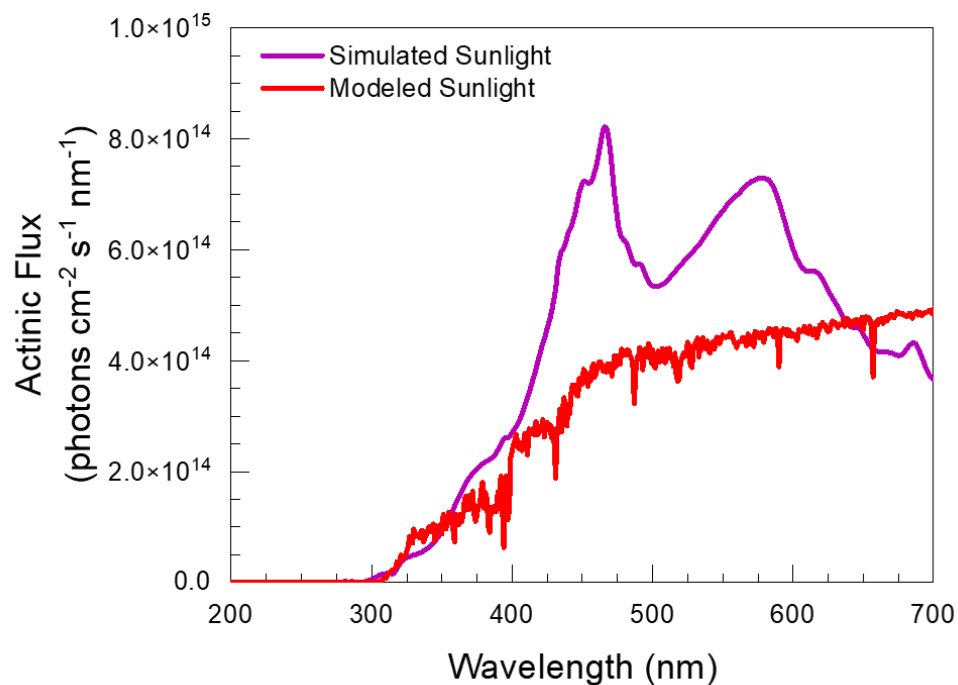


Figure S1. Experimental and simulated actinic flux. The red line is the modeled, midday Davis winter-solstice actinic flux from the Tropospheric Ultraviolet and Visible Radiation Model Version 5.3 (https://www.acom.ucar.edu/Models/TUV/Interactive_TUV/). The purple line is the measured photon flux from our solar simulator on a day with $j_{2NB} = 0.0051 \text{ s}^{-1}$. The solar simulator contains a 1000 W Xe lamp equipped with a downstream water filter, an AM1.0 air mass filter (AM1D-3L, Sciencetech), and a 295 nm long-pass filter (20CGA-295, Thorlabs).

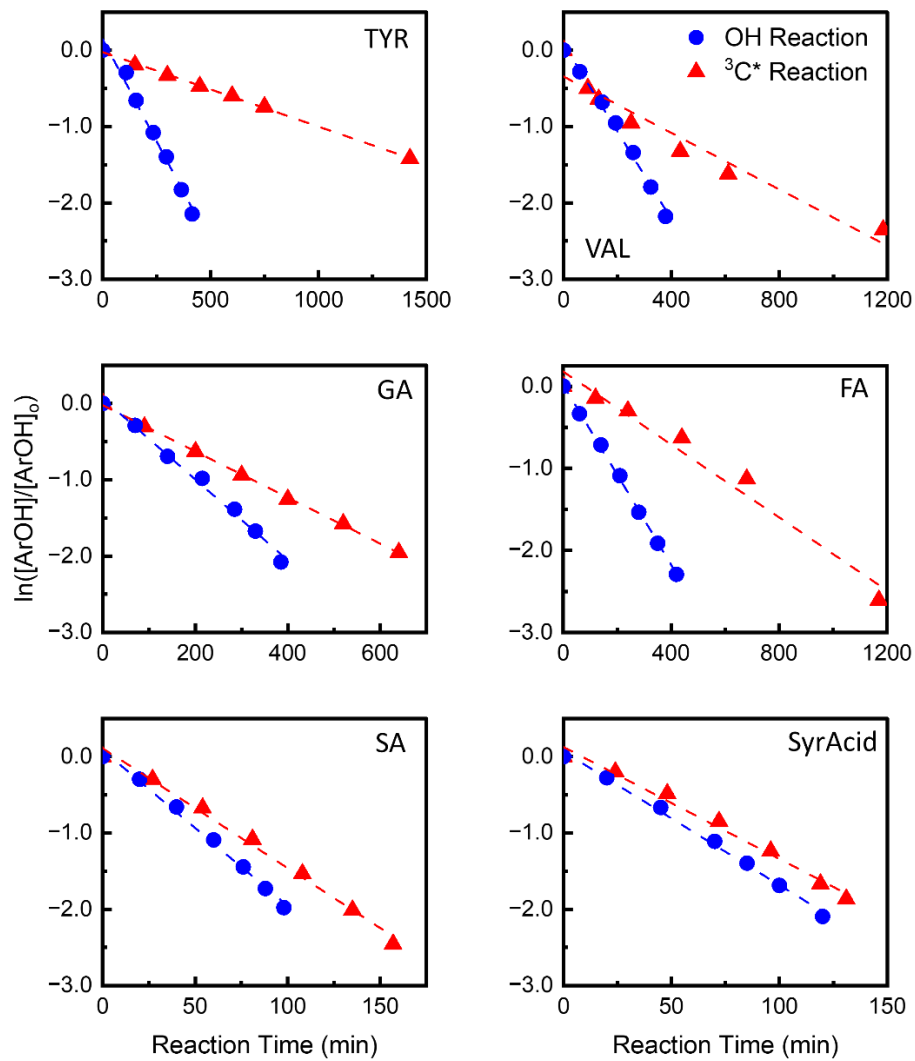


Figure S2. ArOH oxidation kinetics with $\bullet\text{OH}$ (blue circles) and $^3\text{C}^*$ (red triangles).

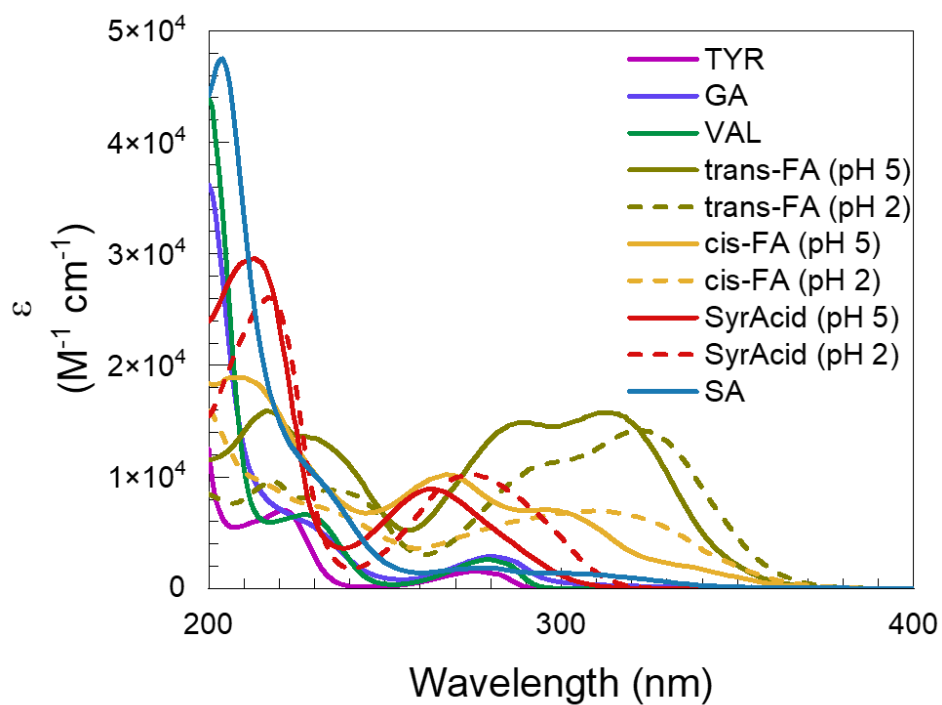


Figure S3. Base-10 molar absorption coefficients (ϵ) for aqueous, highly substituted ArOH. Values, which are tabulated in Table S2, were determined from the spectra of five different solutions of each ArOH at 25 μM , 100 μM , 500 μM , 1.0 mM, and 2.0 mM in a 1 cm cell.

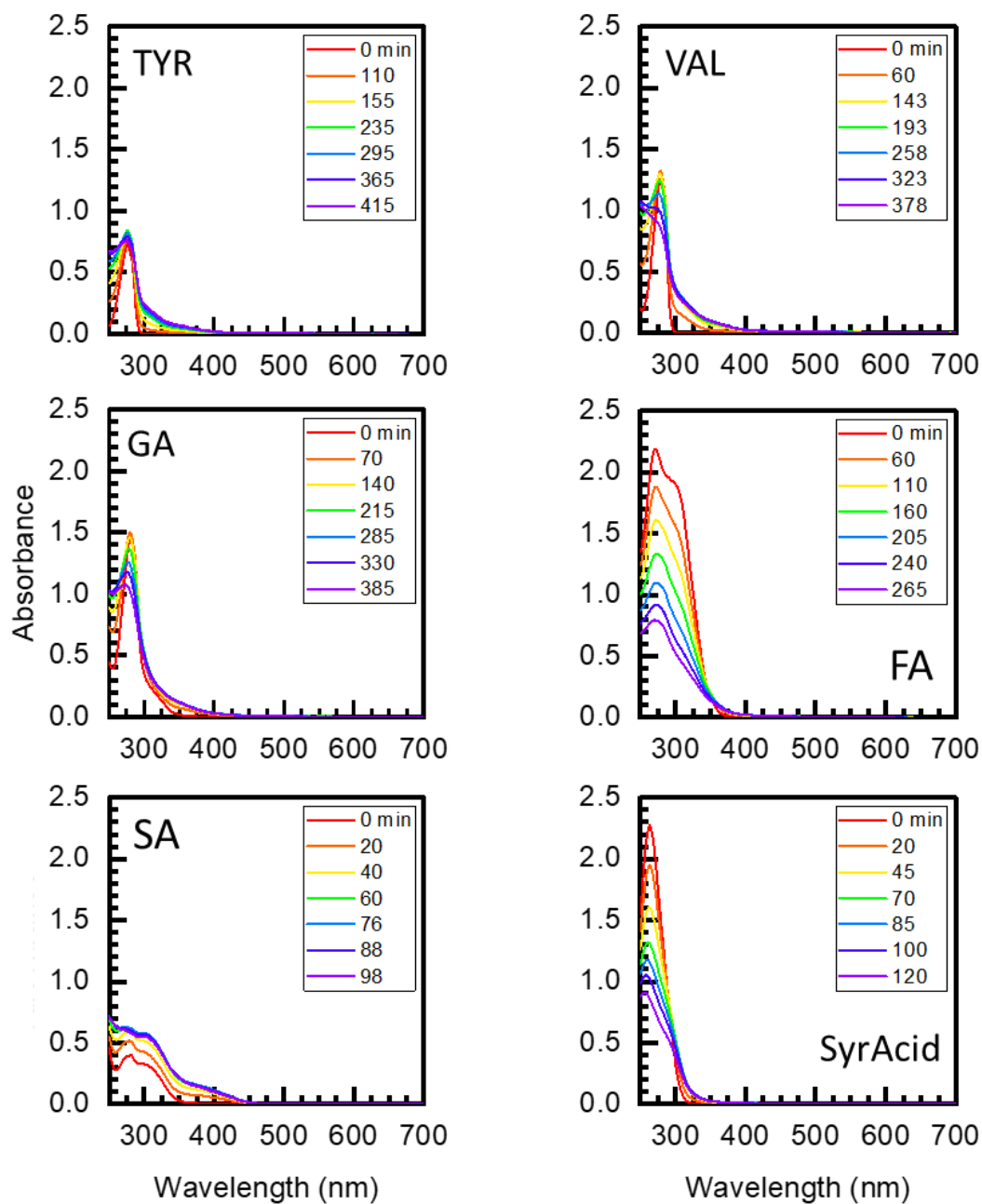


Figure S4. Absorbance measurements for mixtures during the $\bullet\text{OH}$ reactions. The absorbance here, which was measured in a 5-cm cell at each time point, represents contributions from the oxidant precursor, starting phenol, and products.

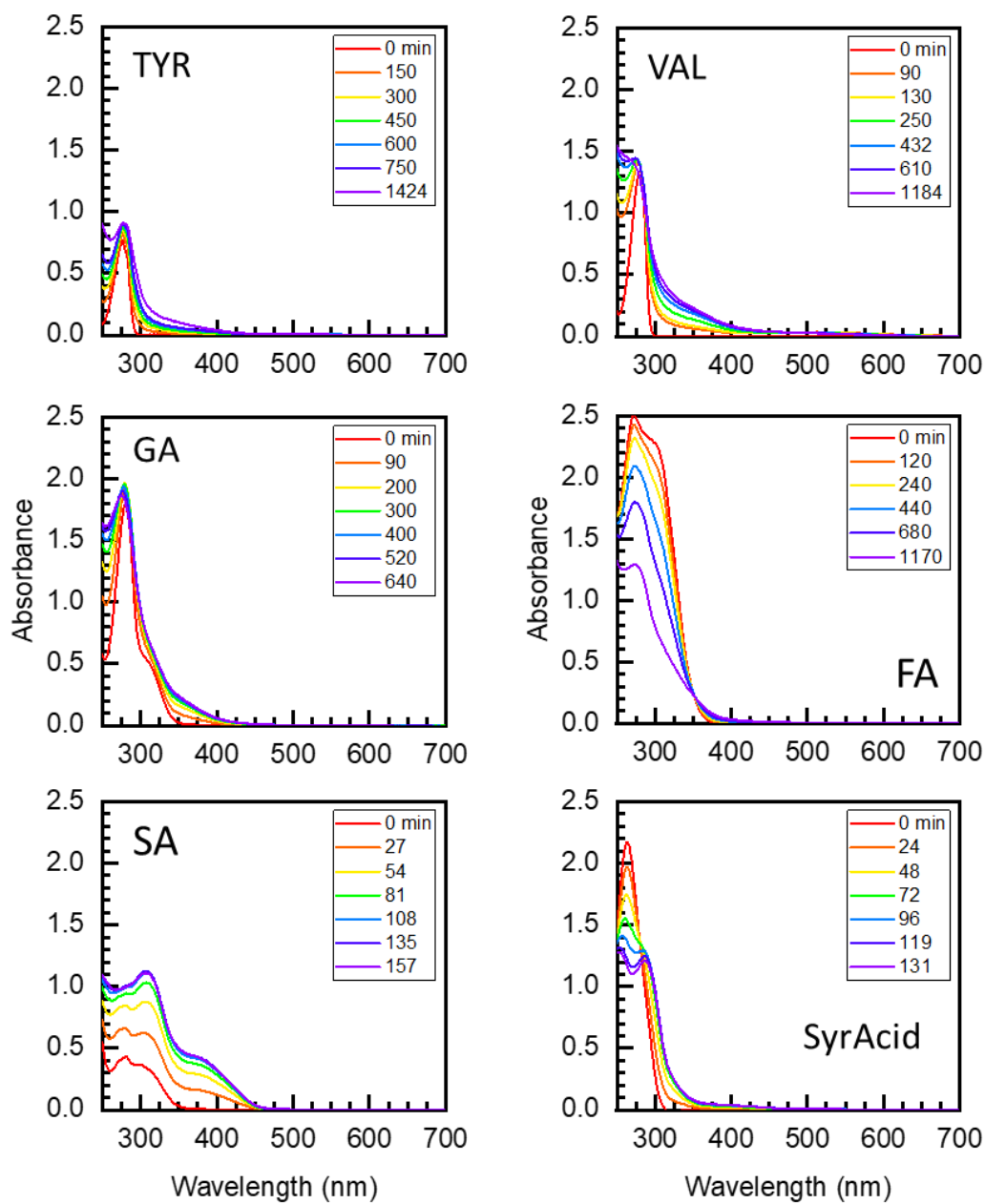


Figure S5. Absorbance measurements for mixtures during $^3\text{C}^*$ reactions. The absorbance here, which was measured in a 5-cm cell at each time point, is due to the oxidant precursor, starting phenol, and products.

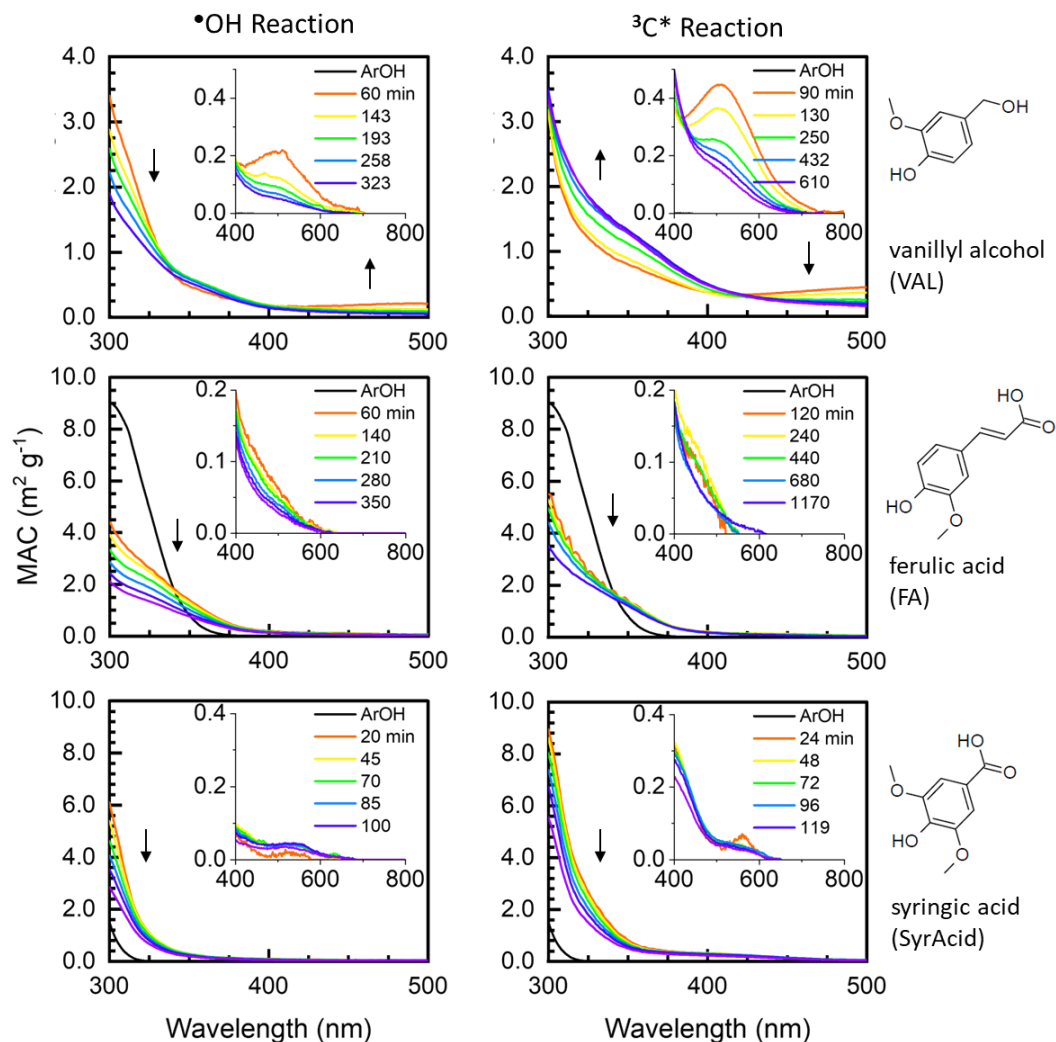


Figure S6. Evolution of mass absorption coefficients (MAC) of aqSOA formed from the $\bullet\text{OH}$ reaction (left column) and $^3\text{C}^*$ reaction (right column) of three phenols: vanillyl alcohol (top pair of panels), ferulic acid (middle pair), and syringic acid (bottom pair). Arrows show the trend in MAC (i.e., increasing or decreasing) in a given wavelength region as a function of illumination time. The MAC value for each starting phenol is shown as a black line. The absorbance contributions of the starting phenol and oxidant precursor (i.e., H_2O_2 or DMB) have been removed from the aqSOA MAC values (colored lines).

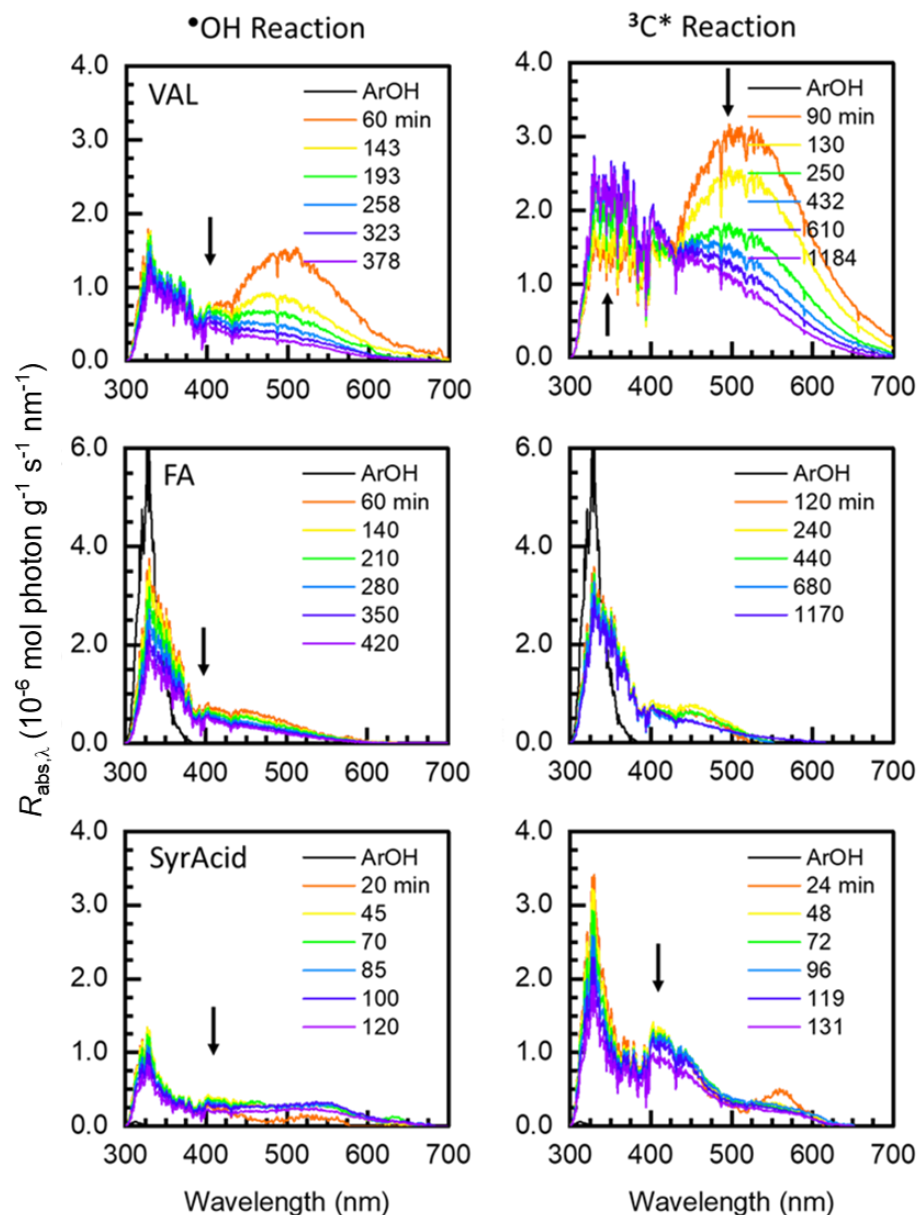


Figure S7. Rates of sunlight absorption for aqSOA formed from vanillyl alcohol (VAL; top), ferulic acid (FA; middle), and syringic acid (SyrAcid; bottom). The left column shows results for reactions of each phenol with $\bullet\text{OH}$ while the right column shows the parallel results for $^3\text{C}^*$ (right column) over the course of illumination. For a given phenol, the black line represents sunlight absorption by the parent ArOH and the colored lines are sunlight absorption for aqSOA at different illumination times. Arrows represent the time trends of aqSOA MAC values after the initial illumination time point.

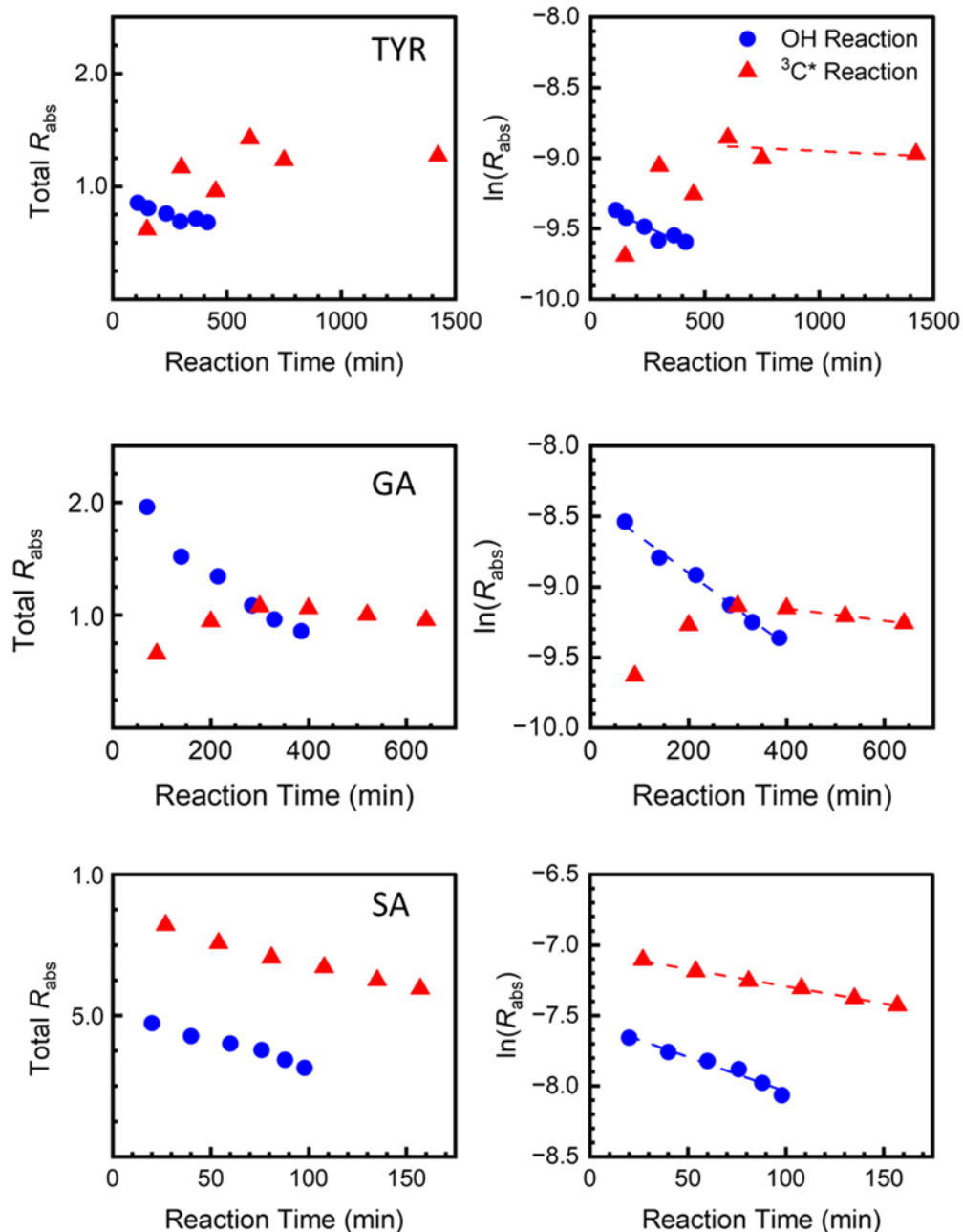


Figure S8. Decay in the rate of sunlight absorption (R_{abs} , $10^{-4} \text{ mol photon g}^{-1} \text{ s}^{-1}$) for aqSOA formed from tyrosol (TYR), guaiacylacetone (GA), and syringyl acetone (SA) during continued reaction. The left column shows the total rate of aqSOA light absorption (from 280 to 800 nm) over the course of each illumination. The right column shows the same data, but with the natural log of the total rate of light absorption; these plots were used to determine the pseudo-first-order decay of light absorption by aqSOA during illumination. Dashed lines indicate the time points used to determine k'_{Rabs} values (Equation 2) for the reactions with triplets (red triangles and lines) and $\bullet\text{OH}$ (blue circles and lines).

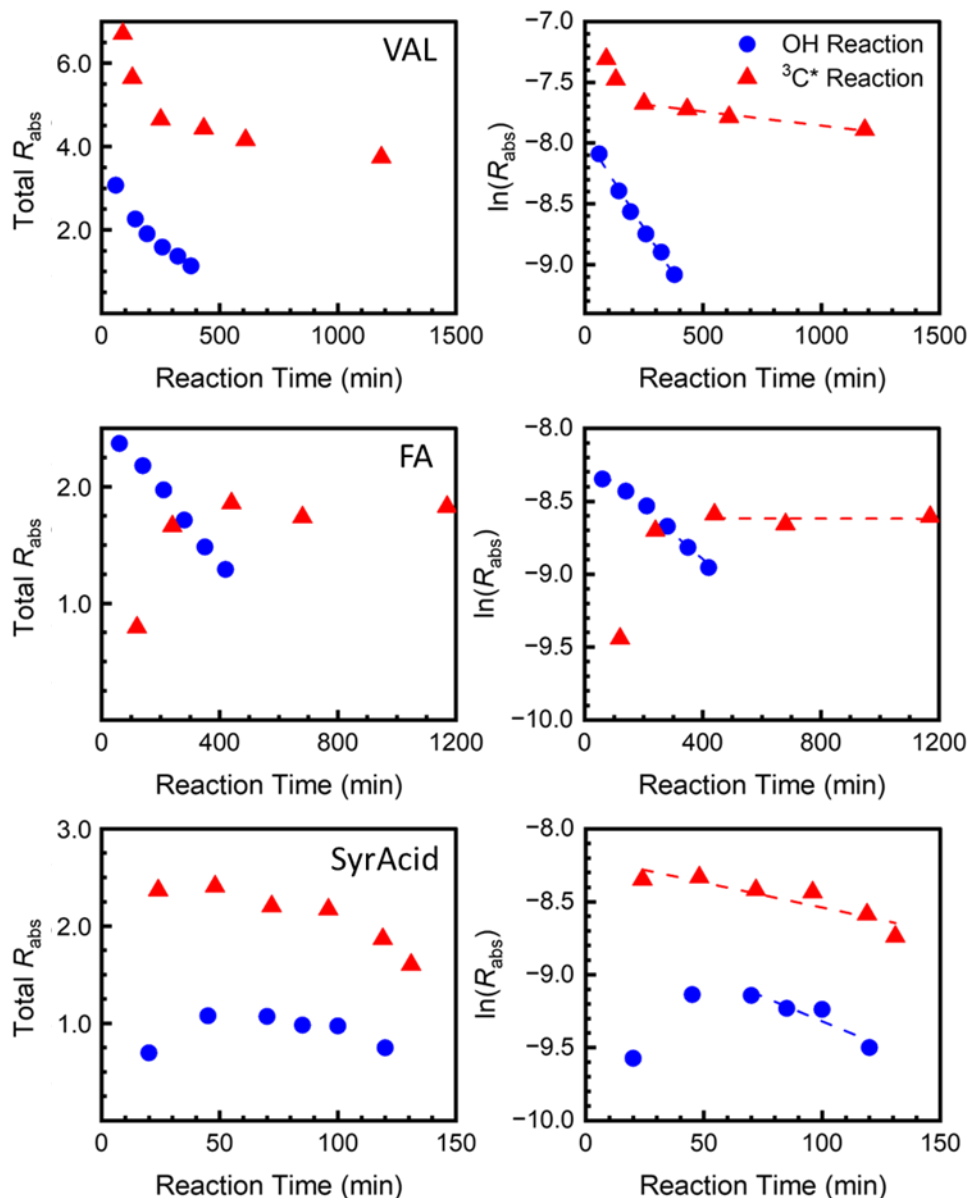


Figure S9. Decay in the rate of sunlight absorption (R_{abs} , $10^{-4} \text{ mol photon g}^{-1} \text{ s}^{-1}$) for aqSOA formed from vanillyl alcohol (VAL), ferulic acid (FA), and syringic acid (SyrAcid). The left column shows the total rate of aqSOA light absorption (summed from 280 to 800 nm) at each sampled time point. The right column shows the same data, but with the natural log of the total rate of light absorption; these plots were used to determine the pseudo-first-order decay of light absorption by aqSOA during illumination. Dashed lines indicate the time points used to determine k'_{Rabs} values (Equation 2) for the reactions with triplets (red) and $\bullet\text{OH}$ (blue).

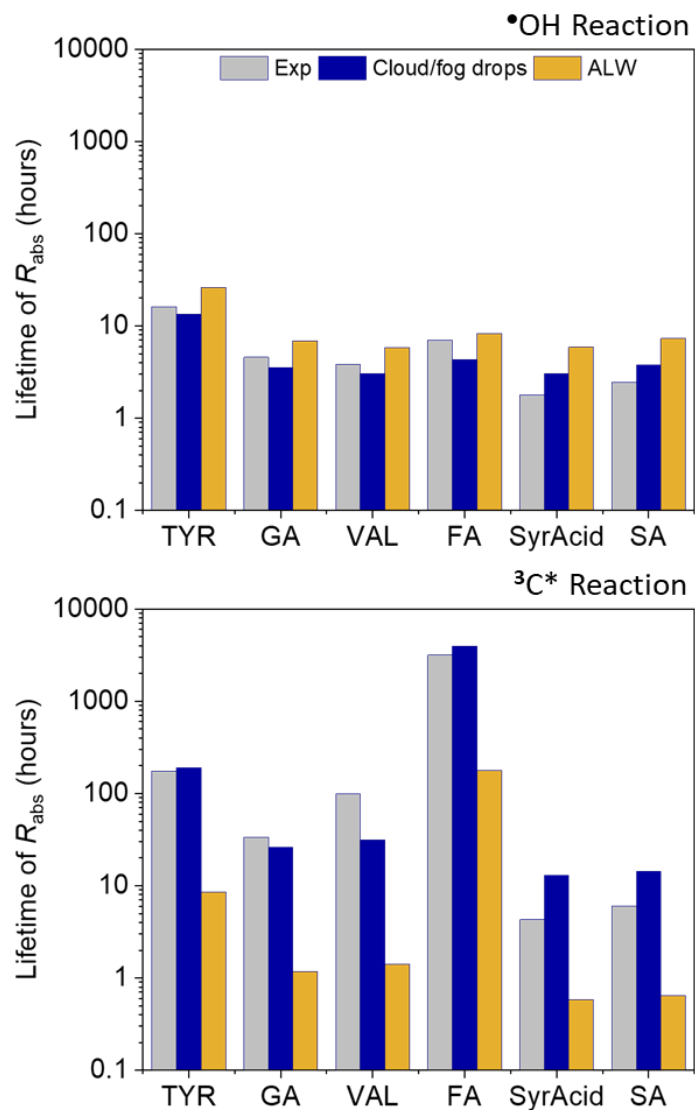


Figure S10. Lifetimes of phenolic BrC formed from $\bullet\text{OH}$ and $^3\text{C}^*$ reactions. Top panel: Lifetimes of the rate of sunlight absorption by $\bullet\text{OH}$ -formed aqSOA with respect to $\bullet\text{OH}$ oxidation under conditions of: (a) our experiments (gray bars), (b) cloud/fog drops (blue bars), and (c) ALW (gold bars). Bottom panel: Lifetime of light absorption by triplet-formed aqSOA with respect to oxidation by triplets.

Section S1. Absorbance correction and MAC determinations for parent ArOH

The experimentally measured absorbance of a reaction mixture at a given wavelength ($Abs_{exp,\lambda}$, e.g., Figures S4 and S5) includes contributions from the starting phenol ($Abs_{ArOH,\lambda}$), H₂O₂ or DMB as the oxidant precursor ($Abs_{Ox,\lambda}$), and the aqSOA that formed ($Abs_{aqSOA,\lambda}$):

$$Abs_{exp,\lambda} = Abs_{ArOH,\lambda} + Abs_{Ox,\lambda} + Abs_{aqSOA,\lambda}. \quad (S1)$$

To calculate the MAC for the parent ArOH (MAC_{ArOH}) in this mixture, we took the absorbance at time 0 (i.e., where $Abs_{aqSOA,\lambda} = 0$) and subtracted the absorbance contribution from the known concentration of either H₂O₂ (in •OH reactions) or DMB (in ³C* reactions):

$$Abs_{ArOH,\lambda} = Abs_{exp,\lambda} \text{ at time zero} - Abs_{Ox,\lambda}, \quad (S2)$$

$$\text{where } Abs_{Ox,\lambda} = \epsilon_{Ox,\lambda} \times [Ox] \times l. \quad (S3)$$

The absorbance of the oxidant precursor at wavelength λ was determined as the product of the base-10 molar absorption coefficient of the precursor ($\epsilon_{Ox,\lambda}$, M⁻¹ cm⁻¹), the oxidant precursor concentration ([Ox], M), and the cell path length (l , cm). Values of the oxidant precursor molar absorption coefficients are from Miller and Kester (1988) for H₂O₂ and from Smith et al. (2014) for DMB.

The remaining absorbance at time 0 represents the absorbance of the starting phenol. Absorbance values for the starting phenol can also be calculated using the molar absorption coefficients from Table S2 and equation S2; this procedure results in the same values.

$$Abs_{ArOH,\lambda} = \epsilon_{ArOH,\lambda} \times [ArOH] \times l \quad (S4)$$

This parent phenol absorbance was then used to calculate the corresponding MAC:

$$MAC_{ArOH,\lambda} (\text{m}^2 \text{g}^{-1}) = \frac{2.303 \times Abs_{ArOH,\lambda} \times 10^3 \times 10^{-4}}{l \times [ArOH]} \quad (S5)$$

where 2.303 converts the absorbance from base-10 to base-e, l is the path length of our cuvette (5 cm), [ArOH] is starting phenol mass concentration (g L⁻¹), the factor of 10³ converts from L to cm³, and the factor of 10⁻⁴ converts from cm² to m².

For subsequent time points, we calculated the wavelength-specific absorbance of aqSOA in the reaction mixture by removing the absorbance contributions from both the remaining parent phenol and oxidant precursor:

$$Abs_{aqSOA,\lambda} = Abs_{exp,\lambda} - (Abs_{ArOH,\lambda} + Abs_{Ox,\lambda}) \quad (S6)$$

The absorbance of the phenol at a given reaction time and wavelength was determined as the product of its concentration (determined by HPLC), the molar absorption coefficient at that wavelength (Table S2), and the cell path length, as shown in equation S4. The absorbance of the oxidant precursor was determined as explained in equation S3. For triplet experiments, the DMB concentration determined in the same HPLC run as the ArOH measurement.

Because we did not measure the H_2O_2 concentration, we estimated $[\text{H}_2\text{O}_2]$ over the course of illumination by considering the stoichiometries of ArOH and H_2O_2 loss during illumination. The main loss of H_2O_2 is through direct photolysis to form $\bullet\text{OH}$ (SR1), while reaction with $\bullet\text{OH}$ (SR3) is a minor path. Based on the rate constants for SR2 and SR3 (Arciva et al. 2022; Christensen et al. 1982), we calculated the percent of $\bullet\text{OH}$ reacting with ArOH or H_2O_2 in each reaction mixture; e.g., for GA, these are 92% and 8%, respectively. Next, we determined the relationships between the change in the number of moles of H_2O_2 ($\Delta n_{\text{H}_2\text{O}_2}$), $\bullet\text{OH}$ formed ($\Delta n_{\bullet\text{OH}}$) and GA (Δn_{GA}) in these reactions.



For this reaction, $\Delta n_{\text{H}_2\text{O}_2} = 0.5\Delta n_{\bullet\text{OH}}$



Based on the relative rates of SR2 and SR3 as fates of $\bullet\text{OH}$, $\Delta n_{\bullet\text{OH}} = \Delta n_{\text{GA}}/0.92$.



Since 2 $\text{HO}_2\bullet$ combine to form 1 molecule of H_2O_2 , we can rewrite SR3 as



Considering the relative importance of SR2 and SR3 as sinks of $\bullet\text{OH}$, we can write the relationship

$$\Delta n_{\bullet\text{OH}} = (\Delta n_{\text{H}_2\text{O}_2}/0.08) \times 2 = \Delta n_{\text{H}_2\text{O}_2}/0.04 \text{ for SR3.}$$

We can then sum the stoichiometric losses of H_2O_2 and $\bullet\text{OH}$ from these reactions to reveal the relationship between the number of moles of H_2O_2 and GA lost:

$$\text{Total } \Delta n_{\text{H}_2\text{O}_2} = 0.5\Delta n_{\bullet\text{OH}} + 0.04\Delta n_{\bullet\text{OH}} = 0.54\Delta n_{\bullet\text{OH}} = 0.54 \times (\Delta n_{\text{GA}}/0.92) = 0.59 \Delta n_{\text{GA}}.$$

$$\text{That is, } \frac{\Delta n_{\text{H}_2\text{O}_2}}{\Delta n_{\text{GA}}} = 0.59, \quad (\text{S7})$$

which indicates that the number of moles of H_2O_2 lost during reaction is 59% of the number of moles of GA lost for our conditions. This example is specific for GA, but we performed parallel calculations for the other five phenols. The percentage for reactions of TYR, GA, and VAL average ($\pm 1\sigma$) to 59% ($\pm 1.0\%$), and for FA, SyrAcid, and SA, 76% ($\pm 4.0\%$). These percentages are different across the two sets of ArOH due to the different starting concentrations of precursor ArOH and H_2O_2 (Table S1).

The ratio of the change in the number of moles in the reaction solution is equivalent to the ratio expressed as concentrations. Thus, we can determine $\Delta[\text{H}_2\text{O}_2]_t$, how much the concentration of H_2O_2 changed between adjacent reaction sampling times, by:

$$\Delta[\text{H}_2\text{O}_2]_t = \Delta[\text{ArOH}]_t \times \frac{\Delta n_{\text{H}_2\text{O}_2}}{\Delta n_{\text{ArOH}}}, \quad (\text{S8})$$

where $\frac{\Delta n_{H_2O_2}}{\Delta n_{ArOH}}$ is 0.59 for GA, $\Delta[ArOH]_t$ is the change in ArOH concentration between two time points as determined by HPLC, and $\Delta[H_2O_2]_t$ is the change in H_2O_2 concentration in M. For use in equation S3 for the $\bullet OH$ experiments, we determined the concentration of H_2O_2 in the reaction solution at a given time using:

$$[H_2O_2]_t = [H_2O_2]_o - \Delta[H_2O_2]_t \quad (S9)$$

After all of this work, our calculations indicate that the change in H_2O_2 concentration over the course of illumination was small ($< 5\%$) in our $\bullet OH$ experiments, but we still accounted for it.

References

Anastasio, C. and McGregor, K. G.: Chemistry of fog waters in California's Central Valley: 1. In situ photoformation of hydroxyl radical and singlet molecular oxygen, *Atmos. Environ.*, 35(6), 1079–1089, [https://doi.org/10.1016/S1352-2310\(00\)00281-8](https://doi.org/10.1016/S1352-2310(00)00281-8), 2001.

Arciva, S., Niedek, C., Mavis, C., Yoon, M., Sanchez, M. E., Zhang, Q. and Anastasio, C.: Aqueous ·OH oxidation of highly substituted phenols as a source of secondary organic aerosol., *Environ. Sci. Technol.*, 56(14), 9959–9967, <https://doi.org/10.1021/acs.est.2c02225>, 2022.

Christensen, H., Sehested, K. and Corfitzen, H.: Reactions of hydroxyl radicals with hydrogen peroxide at ambient and elevated temperatures, *J. Phys. Chem.*, 86(9), 1588–1590, <https://doi.org/10.1021/j100206a023>, 1982.

Erdemgil, F. Z., Sanli, S., Sanli, N., Ozkan, G., Barbosa, J., Guiteras, J. and Beltrán, J. L.: Determination of pK(a) values of some hydroxylated benzoic acids in methanol-water binary mixtures by LC methodology and potentiometry., *Talanta*, 72(2), 489–496, <https://doi.org/10.1016/j.talanta.2006.11.007>, 2007.

Ma, L., Guzman, C., Niedek, C., Tran, T., Zhang, Q. and Anastasio, C.: Kinetics and mass yields of aqueous secondary organic aerosol from highly substituted phenols reacting with a triplet excited state, *Environ. Sci. Technol.*, 55(9), 5772–5781, <https://doi.org/10.1021/acs.est.1c00575>, 2021.

Ma, L., Worland, R., Jiang, W., Niedek, C., Guzman, C., Bein, K. J., Zhang, Q. and Anastasio, C.: Predicting photooxidant concentrations in aerosol liquid water based on laboratory extracts of ambient particles, *Atmospheric Chemistry and Physics*, 23(15), 8805–8821, <https://doi.org/10.5194/acp-23-8805-2023>, 2023a.

Ma, L., Worland, R., Heinlein, L., Guzman, C., Jiang, W., Niedek, C., Bein, K. J., Zhang, Q. and Anastasio, C.: Seasonal variations in photooxidant formation and light absorption in aqueous extracts of ambient particles, , <https://doi.org/10.5194/egusphere-2023-861>, 2023b.

Miller, W. L. and Kester, D. R.: Hydrogen peroxide measurement in seawater by (p-hydroxyphenyl)acetic acid dimerization, *Anal. Chem.*, 60(24), 2711–2715, <https://doi.org/10.1021/ac00175a014>, 1988.

Smith, J. D., Sio, V., Yu, L., Zhang, Q. and Anastasio, C.: Secondary organic aerosol production from aqueous reactions of atmospheric phenols with an organic triplet excited state., *Environ. Sci. Technol.*, 48(2), 1049–1057, <https://doi.org/10.1021/es4045715>, 2014.